Met. Mater. Int., Vol. 21, No. 1 (2015), pp. 118~125
doi: 10.1007/s12540-015-1014-8

Improvement of the Decarburization Rate in Austenitic Stainless Steelmaking

Youngjo Kang[1], Yong Hwan Kim[1], and Ho-Sang Sohn[2,*]

[1]POSCO, Technical Research Laboratories, Gyeongbuk 790-785, Korea
[2]Kyoungpook National University, School of Material Science, Daegu 702-701, Korea

(received date:16 November 2013 / accepted date: 29 April 2014)

In order to enhance the decarburization rate at low carbon content region during the decarburization of molten stainless steel in argan oxygen decarburization, inert gas was blown into top slag and molten steel through a top lance. The carbon content at the end point of the decarburization process was found to reach lower values than conventional levels without the inert gas top blowing. The decarburization rate might be improved, probably due to the disturbance of the slag/metal interface and the dilution of CO gas. The influence of slag in decarburization step on the decarburization and the reduction reactions of chrome oxides in the slag were also experimentally and theoretically investigated by establishing a kinetic model of the decarburization of molten stainless steel under the existence of slag containing chrome oxide. The liquid fraction of the slag appears to be essential for a more effective decarburization reaction. Countermeasures were also proposed to prevent carbon pickup from burnt lime for better slag control.

Keywords: oxide, decarburization, interfaces, mass transfer

1. INTRODUCTION

Modern production of stainless steel consists primarily of EAF (Electric Arc Furnace) - AOD (Argon Oxygen Decarburization) - secondary refining. Here, AOD plays a very important role in stainless steelmaking, and for several decades, it has been a main concern to improve the productivity of the AOD process. Since the most important function of the AOD process is the decarburization of molten stainless steel, it is necessary to promote the decarburization reaction to shorten the AOD process time.

In the early stage of decarburization, the blown oxygen is highly efficient for decarburization because the carbon content is high. The decarburization rate in this stage is controlled by the oxygen blowing rate. Hence, a great deal of effort was focused on how to increase the oxygen blowing rate in the high carbon content region. In the early '80s, oxygen top blowing was improved to increase the oxygen blowing rate, and consequently the decarburization rate [1,2]. For the same reason, various activities such as the additional installation of side blowing tuyeres and appropriate control of vessel vibration were attempted [3].

When carbon content is low, on the contrary, not all of the blown oxygen can contribute to decarburization. Thus, as is widely understood, the decarburization rate diminishes with the decrease in carbon content. Since the process time for a low carbon content region is generally longer than that for a high carbon content region, it is important to improve the decarburization rate in low carbon content region.

Recently, the demand for high quality stainless steels, for instance, low carbon grade stainless steel and duplex stainless steel, is growing dramatically. Since an extended processing time is necessary to remove carbon to such a low content, the decarburization rate in later stages is required to be accelerated. In this region, decarburization is mainly controlled by the mass transfer of carbon in molten steel and the reduction of Cr_2O_3 as shown in Eq. (1).

$$Cr_2O_3(s) + 3\underline{C} = 2\underline{Cr} + 3CO(g) \quad (1)$$

To direct the reaction toward the right-hand side, the partial pressure of CO should be lowered and steel bath is sufficiently stirred. A mixture of inert gas and oxygen is then blown into the low carbon content region of the AOD process. To promote the stirring and dilution of CO gas, one solution is top blowing of inert gas as reported in a previous study [4]. Also there is a lack of systematical understanding of slag condition during AOD decarburization.

In this study, experiments were carried out to find out how to improve the decarburization rate in low carbon content region. The influences of inert gas top blowing and slag condition control were also investigated.

*Corresponding author: sohn@knu.ac.kr
©KIM and Springer

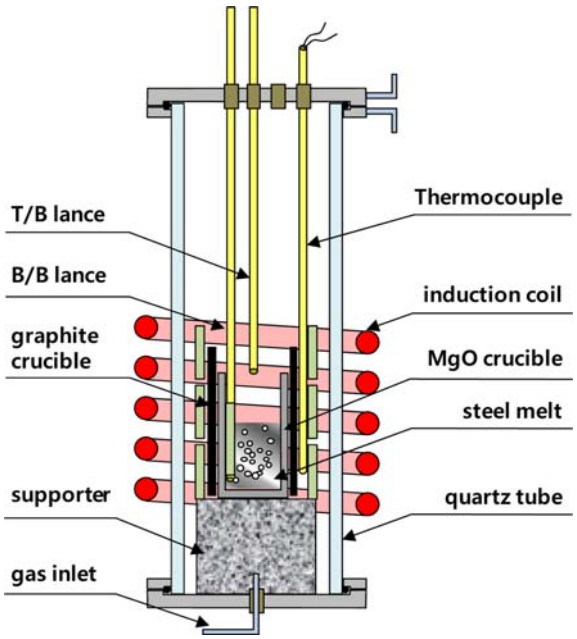

Fig. 1. Schematic representation of experimental apparatus.

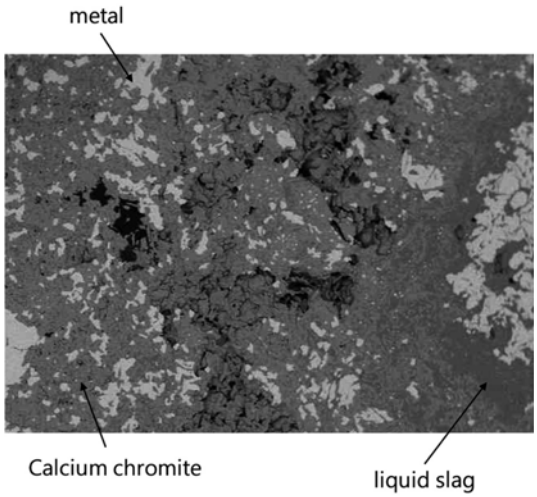

Fig. 2. Typical SEM micrograph of slag formed on stainless steel surface after preliminary experiment.

2. EXPERIMENTS PROCEDURE

To investigate the decarburization behavior of molten stainless steel, a number of lab-scale experiments were carried out. As shown in Fig. 1, an induction furnace equipped with gas inlets for top and bottom blowing was employed in most of the experiments. Steel samples were contained in an MgO crucible located in a graphite heating element. The temperature was controlled at 1,923 K within ± 2 K by means of a thermocouple placed below the graphite heating element.

A preliminary experiment simulating AOD slag condition during decarburization was carried out. About 2,000g of a steel sample, with an initial composition of 2 wt%C-18 wt%Cr-8 wt%Ni-0.2 wt%Si, was melted in an induction furnace. Once molten, various amounts of burnt lime were introduced. Argon and oxygen gas (20 cm^3/sec) were blown at the bottom and top of the molten steel, respectively. After about 20 min, slag formed on the molten steel and samples were taken. The samples were cross-sectioned and carefully examined by a Scanning Electron Microscope (SEM) and one micrograph is presented in Fig. 2. Note that the slag primarily consists of a compound of Cr oxide and CaO and a small volume of liquid slag containing CaO and SiO_2. In actual AOD practice, it can be expected that large amount of calcium chromite is present after oxygen top blowing. This Cr oxide compound plays an important role in the decarburization in low carbon content region.

2.1. Inert Gas Top Blowing

The influence of top blowing on the decarburization by Cr oxide in low carbon content region was investigated.

The initial composition of steel was adjusted to be 0.2 wt%C-18 wt%Cr-8wt%Ni using pig iron and reagent grade metallic Cr and Ni. After melting 2,000 g of stainless steel, a lance for bottom bubbling was inserted into the molten steel with about 10 mm clearance from the bottom of the crucible. Argon gas or Ar+O_2 were selected for the bottom blowing gas and introduced at a flow rate of 10 cm^3/sec in most cases. The oxygen partial pressure of the bottom blown Ar+O_2 mixture gas was controlled to be 0.2 atm. In some experiments, Ar gas was blown through a top lance at a rate of 20 or 30 cm^3/sec.

Once the steel sample was molten, the system was kept with only bottom blowing of Ar gas for 4-5min to ensure uniformity. After the initial sample was taken, the bottom blowing gas was switched as needed. About 40 g of synthetic solid slag were introduced into the molten steel at $t = 0$ min. The slag was prepared by sintering pellets with a composition of 30 wt%CaO-70 wt%Cr_2O_3, as confirmed by preliminary examination, and then crushed into grains smaller than 2 mm. The blowing time was approximately 90 min, and steel samples for chemical analysis were taken by quartz tubes at 5 min intervals.

2.2. Control of Slag during Decarburization

The influence of slag in low carbon content region on decarburization was also investigated.

Although the experimental procedure was more or less the same as described in the previous section, three different types of synthetic slag-CaO·Cr_2O_3, pure Cr_2O_3, and calcium silicate liquid slag with a small content of Cr_2O_3 were employed. Reagent grade chemical (99.99% purity) was used for Cr_2O_3 and liquid slag with a composition of 55 wt%CaO-35 wt%SiO_2-10 wt%Cr_2O_3 was prepared by premelting, respectively. For each type of slag, the input amount was determined, so that the amount of Cr_2O_3 is equivalent. After the slag was introduced, gas blowing was carried out in the pre-determined manner, and steel samples were taken in every 5 min for chemical analysis.

Table 1. Composition of stainless steel used in carbon pick-up experiments

	C	Si	Cr	Ni
wt%	0.05	0.4	18.0	8.0

On the other hand, the influence of changes in liquid fraction in slag on the decarburization was investigated by adding liquid phase formers, such as the premelted slag specified in the previous section and SiO_2, into the $CaO.Cr_2O_3$ slag.

2.3. Carbon Pick-up from Burnt Lime

In stainless steel production, a large amount of burnt lime is used for desulphurization and protection of refractory material. There is doubt, however, that CaO is a source of carbon pick-up, particularly in low carbon grade steel production. CaO is generally produced by the calcination of limestone for the removal of CO_2, which may be the carbon source if it remains in the core of CaO.

A series of experiments were carried out to investigate the effect of the residual CO_2 in CaO on carbon pick-up in molten stainless steel. About 1,000 g of stainless steel ingot, whose composition is presented in Table 1, was melted in a similar manner as described in the previous section. After the target temperature was achieved, limestone (CaO > 54 wt%), that is calcium carbonate, was introduced into the steel sample. A number of steel samples were taken at time intervals to analyze changes in carbon content under various conditions of limestone, such as the amount and size. The size of limestone was classified into 4 groups, i.e. A: 0.475~0.9 cm, B: 0.17~0.475 cm, C: 0.09~0.17 cm, D: ~0.09 cm (ave. 0.006 cm). And the amounts of limestone were adjusted to be about 8.6 g, 4.3 g and 2.2 g. To determine a clearer mechanism of carbon pick-up, the reacted surface steel sample was carefully examined by an electron microscope, and the influences of liquid slag and inert gas blowing were also considered.

The contents of [C], [O] and [Cr] in steel samples taken during the experiments were quantified by carbon/sulphur analyzer, oxygen/nitrogen determinator, and XRF, respectively. Slag composition was determined by XRF after glass beading and wet chemical analysis.

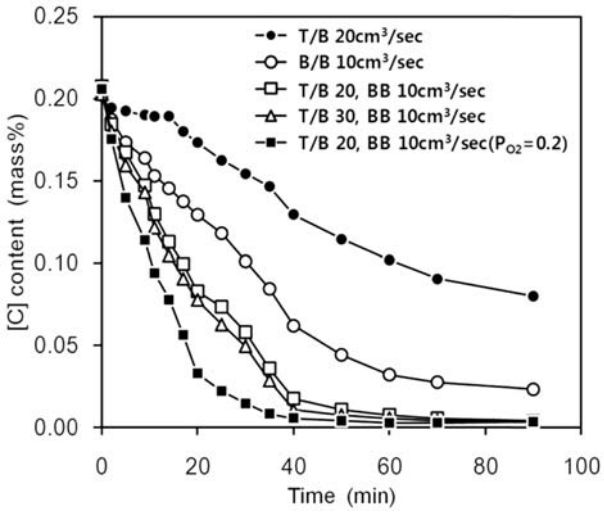

Fig. 3. Decarburization behavior by Cr oxide under various blowing conditions.

3. RESULTS AND DISCUSSION

Among a series of decarburization experiments by slag under various blowing conditions, a few experiments in Table 2 are selected to investigate the effects of experimental conditions, such as types of slag, blowing conditions, and liquid phase in the slag.

3.1. Effect of Inert Gas Top Blowing on Decarburization

The decarburization behavior in low carbon content region was investigated with only bottom blowing and top-bottom combined blowing of inert gas.

Figure 3 represents the change in carbon content of molten stainless steel during the decarburization by $CaO{\cdot}Cr_2O_3$ under various blowing conditions. When oxygen gas was blown from the bottom, the carbon content decreased most rapidly. This result could be expected because blown oxygen can easily contribute to decarburization. Among the cases where oxygen was supplied from Cr oxide and only inert gas was blown, the decarburization with top and bottom combined

Table 2. Selected conditions of decarburization experiments by slag

	Metal(g)	Slag (g)				Bottom blown gas (cm^3/min)	Top blown gas (cm^3/min)
		Cr_2O_3	$CaO{\cdot}Cr_2O_3$	CSK*	SiO_2		
Blowing1	2,000	-	25	-	-	0, 10 (P_{O2}=0, 0.2)	0, 20, 30
Blowing2		-	-	100	-	0, 10 (P_{O2}=0, 0.2)	0, 20, 30
Slag1	500	50	-	-	-	0~15 (P_{O2}=0, 0.2)	-
Slag2		10	-	-	-	0~15 (P_{O2}=0, 0.2)	-
Slag3		-	10	-	-	0~15 (P_{O2}=0, 0.2)	-
Slag4		-	-	50	-	0~15 (P_{O2}=0, 0.2)	-
Liquid1	2,000	-	20	50	-	0, 10 (P_{O2}=0, 0.2)	20
Liquid2		-	25	-	17	0, 10 (P_{O2}=0)	20

*CSK: $CaO\text{-}SiO_2\text{-}Cr_2O_3$

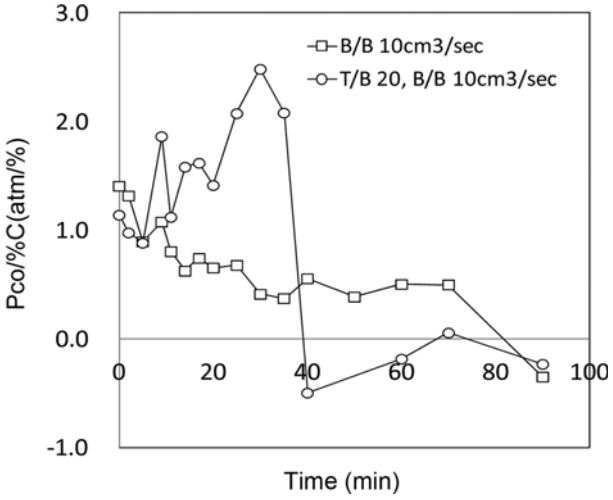

Fig. 4. Changes in the ratio of the partial pressure of CO against carbon content in molten steel.

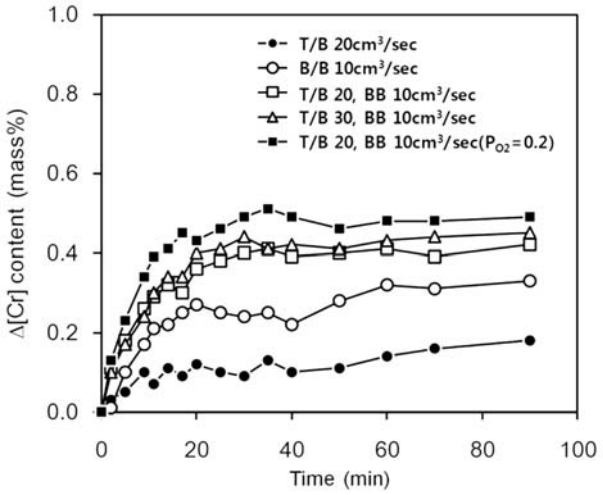

Fig. 5. Changes in chromium content during decarburization under various blowing conditions.

blowing turned out to be the fastest, compared to top or bottom single blowing. Especially, top blowing only did not contribute to decarburization as much as bottom blowing only. The flow rate of top blowing was not so effective on the decarburization when only top blowing was used; however, the higher flow rate of top blowing combined with bottom blowing resulted in a higher decarburization rate.

To understand why the top and bottom combined blowing results in a better decarburization rate, the effect of P_{CO} on decarburization was considered. The decarburization rate is known to be proportional to the difference between the equilibrium and the real carbon content. This can be further inversely expressed with the ratio of the partial pressure of CO gas over the carbon content, which can be regarded as an index of 'suppressing tendency for the decarburization', as previously explained. In Fig. 4, the dynamic values of the ratio of the partial pressure of CO gas over the carbon content during the experiments were presented to compare the results of single bottom blowing and top and bottom blowing. Up to about 40 min., in the case of the estimated P_{CO} value, the single bottom blowing seemed to be favorable for the decarburization rate compared to the combined blowing. The disagreement could occur when the actual P_{CO} is much lower than the estimated P_{CO}, due to flushing by the top blowing. Another explanation could be that the stirring of the top slag and molten steel by the bottom blowing is more effective than the top blowing only.

During decarburization, the chromium content in molten steel increases, due to the reduction of Cr oxide. As shown in Fig. 5, the chromium content increases as the decarburization proceeds and becomes rather constant once the carbon content becomes very low. During the faster decarburization rate in the early stage, greater amounts of Cr oxide are reduced and picked up in the molten steel.

3.2. Effect of Slag Conditions on Decarburization

Since it was found that the slag that formed on the molten steel surface in the simulated experiments for the AOD process consists of mostly $CaO{\cdot}Cr_2O_3$, the calcium chromite was considered as a slag during decarburization in the previous section. However, $CaO{\cdot}Cr_2O_3$ can be thought to be unfavorable to be reduced because of the relatively high melting point and low activity of Cr_2O_3.

After stainless steel, with an initial carbon content of 0.2 wt%, is melted, specific amounts of three types of slag were introduced onto the molten steel surface. The amount of slag was determined so that the net amount of oxygen in Cr_2O_3 was equivalent in each case. The molten steel bath was moderately stirred by Ar bottom blowing with approximately 0.6NL/min per 1 kg of molten steel sample. Typical changes in carbon, oxygen and chromium levels in the steel sample are represented in Fig. 6. As soon as slag is added, carbon content rapidly decreases, while chromium content increases, caused by the decarburization by Cr oxide. As shown in Fig. 6, the decarburization rate for pure Cr oxide or liquid slag (the CaO-SiO_2-Cr_2O_3 system) appeared to be much higher than that for calcium chromite, as mentioned in the previous section.

The decarburization behaviors of the different slag types containing Cr_2O_3 are compared in Fig. 7. Obviously, the decarburization by pure Cr_2O_3 and liquid slag is far more effective than for solid $CaO{\cdot}Cr_2O_3$. It is an indication that $CaO{\cdot}Cr_2O_3$ is too stable a compound to be reduced, compared to other types of slag. There is only a slight difference between pure Cr_2O_3 and liquid slag containing Cr_2O_3 and the decarburization efficiency of the slag is sufficient or even better than that of oxygen gas.

One of the authors proposed a decarburization model of molten iron under $Ar+O_2$ mixture gas blowing [5]. In the study, a model was verified to be applicable in a wide carbon con-

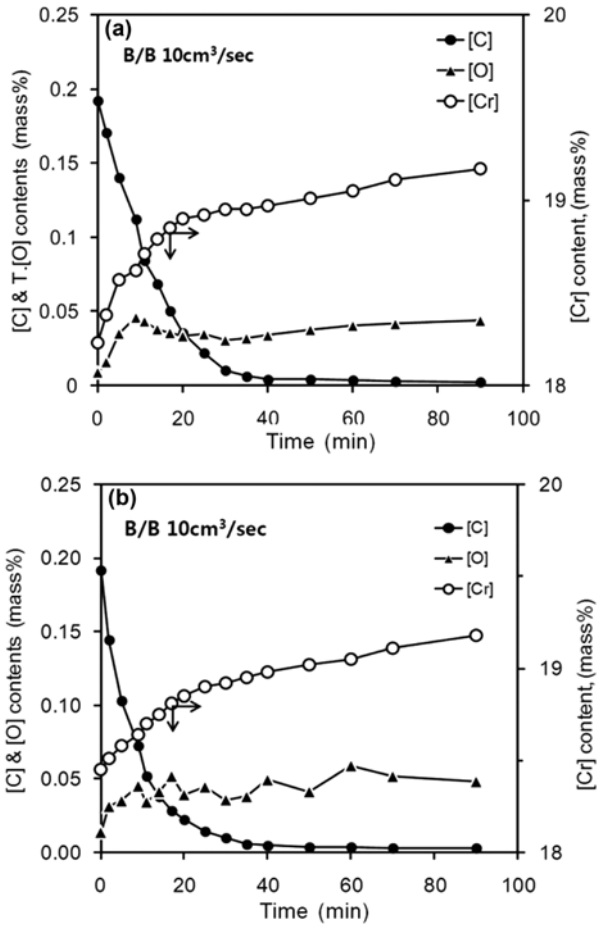

Fig. 6. Changes in carbon, oxygen, and chromium content during decarburization by Cr_2O_3 (a) and $CaO\text{-}SiO_2\text{-}Cr_2O_3$ slag (b).

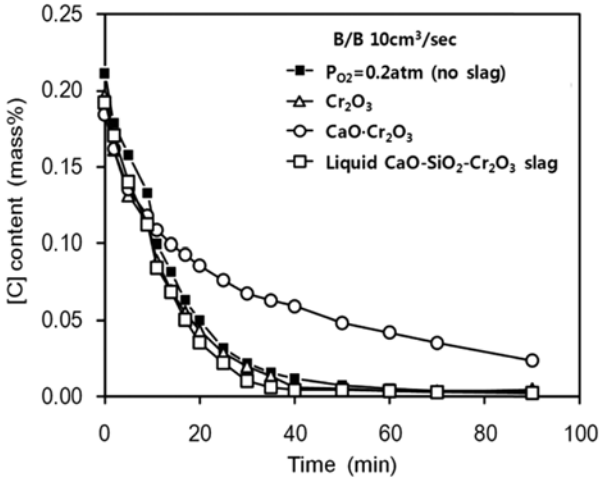

Fig. 7. Comparison of decarburization behaviors under various slag conditions.

tent region, because a mixed rate controlling mechanism in the reaction boundary layer was employed. Similarly, the concept of a boundary layer between two phases - slag and molten steel - was applied to interpret the decarburization by the reduction of Cr oxide in the present study. In molten steel and slag layers, the rate of mass transfer of Cr in the molten steel and Cr_2O_3 in the slag was estimated when both were stirred by bottom blown inert gas. Adopting the partition ratio of chromium in the two phases, the change in chromium contents in the molten steel with time could be predicted. Subsequently, the mass transfer coefficients of Cr in the molten steel and Cr_2O_3 in the slag could be determined by a comparison of the predicted and measured results. Compared to the mass transfer in the molten steel, the mass transfer in the slag seems to be far more influential on the rate of decarburization reaction by Cr_2O_3 in the slag. When more liquid phase in the slag exists, the mass transfer coefficient of the Cr_2O_3 in slag appeared to be much improved, as shown in Fig. 8. It was also found that the mass transfer in slag could be slightly improved by modifying the flow rate of the top blowing.

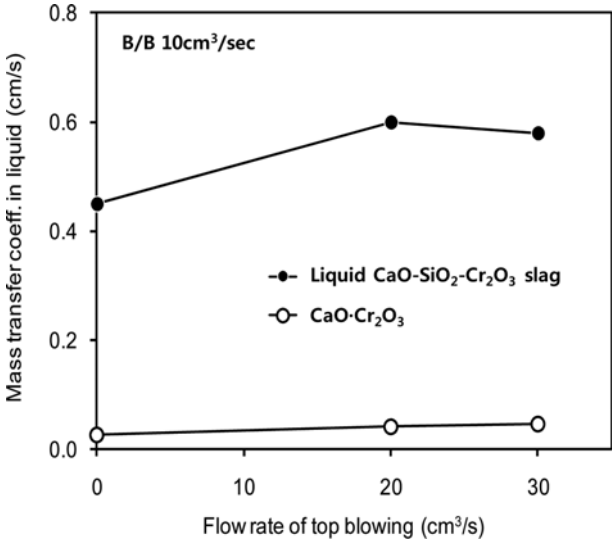

Fig. 8. Mass transfer coefficient in liquid $CaO\text{-}SiO_2\text{-}Cr_2O_3$ slag and $CaO{\cdot}Cr_2O_3$ solid slag.

Nonetheless, large amount burnt lime is added in industrial practice for desulphurization and the protection of refractory material. Hence, it is hardly possible that Cr oxide formed by oxygen blowing remains pure Cr_2O_3. To improve decarburization efficiency, therefore, it will be essential to form liquid slag rather than solid calcium chromite. A solid phase related to Cr_2O_3 will be inevitably formed during decarburization of molten stainless steel; however, a greater liquid fraction of the slag during decarburization should be pursued. For instance, it can be an appropriate practice to use the additives to promote the melting of slag, such as SiO_2, although the limitation of the liquid fraction of the slag may be encountered in practical situations, due to operational problems, such as refractory erosion. In Fig. 9, the decarburization behaviors are shown when additional fluxes were added to $CaO{\cdot}Cr_2O_3$ solid slag. As shown in the figure, from the moment of the addition of

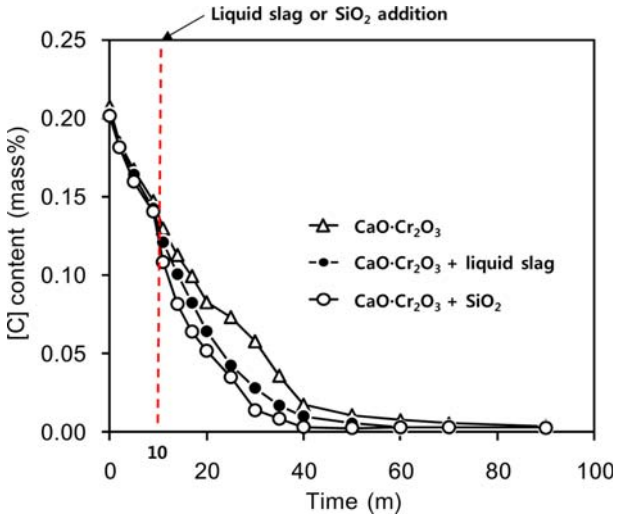

Fig. 9. Decarburization behavior by $CaO·Cr_2O_3$ when fluxes for slag melting were added.

flux to lower the melting point or slag basicity, the decarburization rate increased due to the increase of the liquid fraction of slag, and consequently, the mass transfer coefficient in slag.

3.3. Carbon Pick-up from Burnt lime

In stainless steel production, carbon pick-up from residual CO_2 in burnt lime must be properly controlled. is a concern. Particularly, in the production of stainless steel grades with low carbon content (≤0.02 wt%), even a small amount of carbon pick-up may cause serious problems because a large amount of CaO is usually added in a practical AOD process.

As explained in the previous section, limestone was added to a steady bath of molten steel, and the change in carbon content was analyzed. As soon as the limestone was added to the molten steel, strong fumes were emitted for a time, and particles sometimes congealed on the tranquil steel surface. Analysis revealed that the carbon content drastically increased with the limestone addition. Some of the carbon pick-up behaviors by limestone addition are represented in Fig. 9. While, when a certain amount of Group B was added, it was observed that the carbon content initially increased and was saturated around 70 min as shown in Fig. 10(a), carbon content monotonically increased with time as shown in Fig. 10(b) by the addition of Group C with the same amount as Fig. 10 (a) case. Figure 10(c) demonstrates that the carbon content only increased slightly when a small amount (about 1/4 of Fig. 10(a) case) of Group B was added.

Although the behaviors of carbon pick-up appeared to vary somewhat considering the conditions of size and amount limestone, great difficulty was encountered in controlling the conditions during the experiment due to the breakdown and adhesion of limestone. No clear tendency of carbon pick-up with these conditions was observed. In fact, the carbon pick-

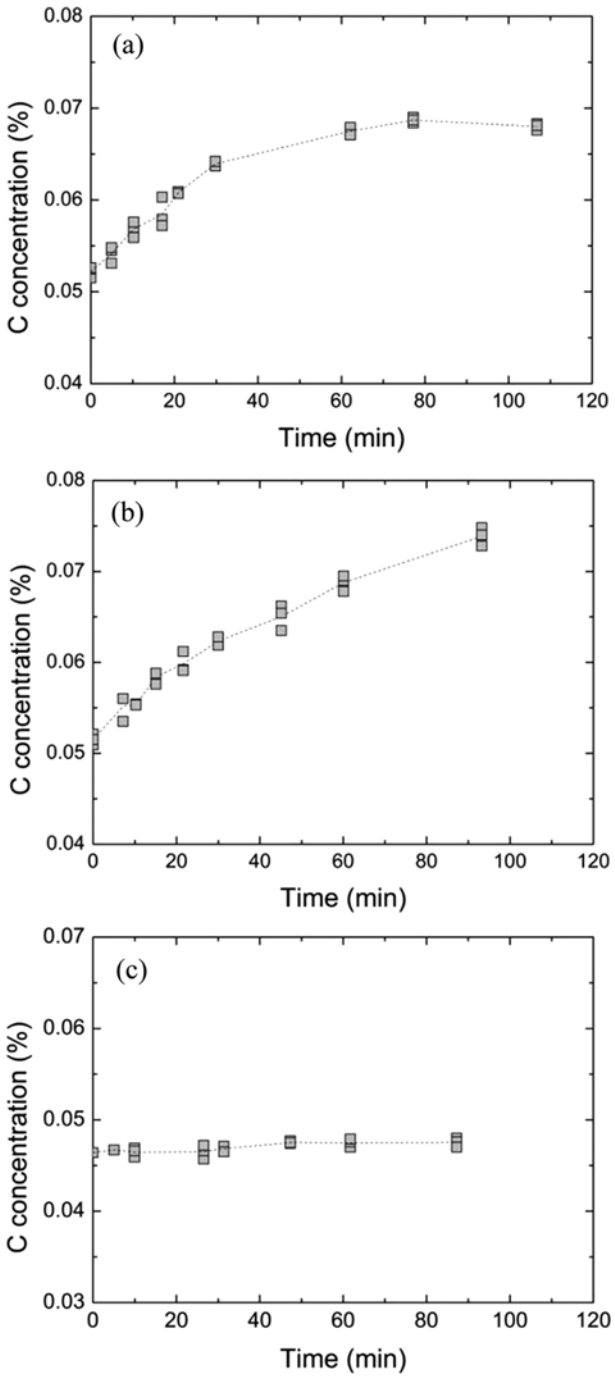

Fig. 10. Carbon pick-up behaviors when limestone with (a) 8.6 g, Group B, (b) 8.6 g, Group C, and (c) 2.2 g, Group B were added.

up behaviors at the very early stage just after of the addition of limestone, when the initial conditions were maintained, may be meaningful. Therefore, the rate of carbon pick-up for 5 min after the addition of limestone was considered. At each condition, the carbon pick-up rate just after the limestone addition and the estimated surface area of limestone, considering the added amount and average size, are tabulated in Table 3; and the relationship between the net surface area of

Table 3. Carbon pick-up rate in the early stages under various conditions of limestone

No.	Size group	Average size (cm)	Amount (g)	Net surface area (cm^2)	Pick-up rate (ppm/sec)
1	B	0.323	8.6	59.04	0.0465
2	B	0.323	8.6	59.04	0.0302
3	A	0.688	8.6	27.70	0.0329
4	C	0.130	8.6	146.47	0.0752
5	D	0.060	8.6	317.34	0.1117
6	B	0.323	4.3	29.52	0.0268
7	B	0.323	2.2	15.10	0.0099

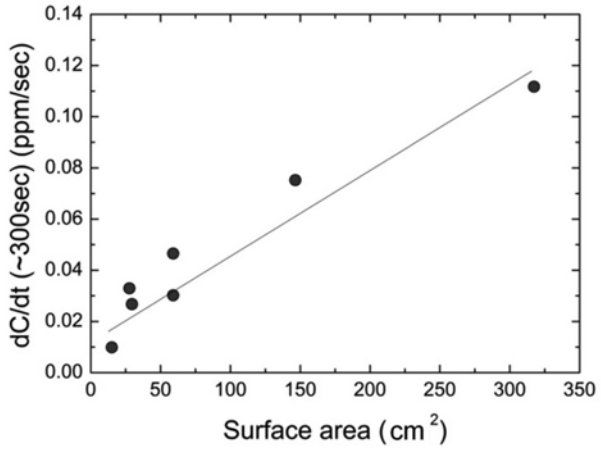

Fig. 11. Relationship between the net surface area of limestone and the rate of carbon pick-up just after limestone addition.

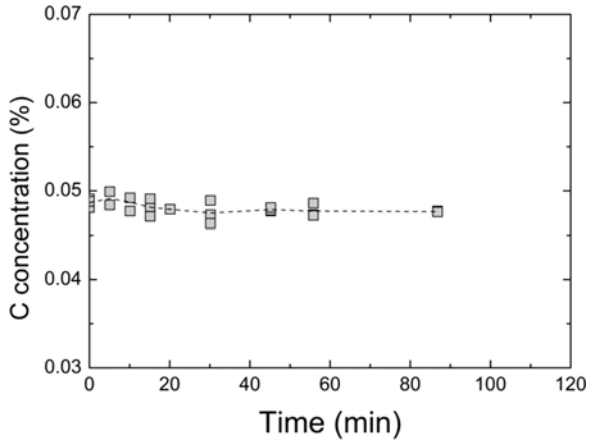

Fig. 12. Carbon pick-up behaviors when limestone with 8.6 g, Group B was added to pre-existing liquid slag.

limestone and carbon pick-up rate in the early stage is plotted in Fig. 11. As shown in the figure, fairly good linearity could be obtained.

The calcination of limestone has been researched in the fields of refractory and iron making for many years. According to one of the most relevant works on the thermal decomposition of limestone [6], the radius shrinking rate of uncalcined core (*dr/dt*, where *r* stands for radius of uncalcined limestone) is constant with time and the decomposition rate of limestone (*dW/dt*, where *W* stands for mass of decomposed limestone) is proportional to *dr/dt* as expressed in the following equation (Eq. 2).

$$\frac{dW}{dt} = \rho \cdot 4\pi r^2 \cdot \frac{dr}{dt} \tag{2}$$

where, ρ stands for limestone density, whose porosity is assumed to be zero. According to the authors, since the amount of decomposition seems to be proportional to the surface area of limestone, it is inferred that the carbon pick-up rate is directly dependent on the decomposition rate of limestone, rightly the formation rate of CO_2. It means that the carbon pick-up might be controlled by the formation and supply of CO_2, even if it should be considered how large a portion of CO_2 will escape without the reaction.

By careful examination on the interface between steel and CaO, which may be partly limestone, a CaO-SiO_2 phase was observed at the interface. Considering the change in oxygen and silicon content, SiO_2 is expected to be formed from the oxidation by CO_2 rather than soluble oxygen. A simple calculation verified that SiO_2 is more stable than CO_2 in the present condition. In other words, carbon can be picked up by molten steel with the oxidation of its metallic elements, mainly silicon.

To restrain the pick-up of carbon from CO_2, therefore, blocking the contact between CO_2 and molten steel will be very effective. For example, the slag layer on molten steel is expected to protect the molten steel from CO_2 emitted from burnt lime. In the simulation experiment shown in Fig. 12, the carbon content did not increase, contrary to previous experiments without slag, when the same amount of limestone (Group B) was added onto the sufficient amount of liquid slag that exists on molten steel. It can be suggested that the application of slag followed by burnt lime addition is very useful to avoid carbon pick-up. A slightly different suggestion about the C pick-up from CaO has been made by Song *et al*. [7] The authors proposed that the deoxidizing agent in the reduction period mostly reacts with carbonate ions in the decarburization slag, which was originated from the residual CO_2 of the CaO. The C content change in AOD slag before and after the reduction period in their research, however, seems to be insufficient for the C pick-up amount in some practical cases,

particularly in low carbon grade steel. Therefore, it is reasonable to consider that a significant amount of the residual CO_2 remaining in the core of CaO may be released only when liquid slag is formed to dissolve its outer shell. Then most of the released CO_2 is expected to be immediately reduced and picked up into molten steel. In this sense, on the contrary, the existence of top slag may efficiently prevent C pick-up.

4. CONCLUSION

Through a number of lab-scale experiments, the decarburization behavior of stainless steel in the AOD process was investigated. Technical possibilities to improve the decarburization rate in low carbon content region were also considered.

Careful analyses and examinations resulted in several findings listed below.

(1) Top blowing of inert gas, combined with bottom blowing could improve the decarburization rate because slag containing Cr oxide and molten steel can be effectively mixed and CO gas can be diluted by the inert gas top blowing.

(2) Under the same blowing conditions, liquid slag as well as pure Cr_2O_3 were much more favorable for decarburization than $CaO{\cdot}Cr_2O_3$ solid slag, which is expected to exist on molten steel surfaces in the AOD process. Calcium chromite is expected to be relatively difficult to be reduced and mass transfer in the liquid slag was faster than that in the solid slag, which was verified by some model prediction of decarburization,

(3) To improve the rate of decarburization, it is very important to increase the liquid fraction of slag in industrial practice. It was found that additives contributing to slag melting, such as silicate slag, are effective in promoting decarburization.

(4) From a number of simulation experiments with limestone, it was confirmed that the residual CO_2 in CaO can be a source of carbon pick-up by molten steel. The rate of carbon pick-up in the early stage was controlled by the net surface area of limestone, similar to its decomposition rate.

(5) It was also noted that carbon is mostly picked up by molten steel through the oxidation of metal elements in steel through the reduction of CO_2. To avoid steel-CO_2 gas contact and minimize carbon pick-up, a sufficient amount of slag on the steel surface can be helpful, as was shown experimentally.

ACKNOWLEDGEMENT

The authors are grateful to Mr. Yong-Ik Jang, who enthusiastically participated in most experiments and contributed to obtaining these results.

REFERENCES

1. H. Okajima, T. Nagahata, Y. Ieda, and M. Yokoyama, *Tetsu-to-Hagane*, **69**, S876 (1983).
2. Y. Kato, T. Fujii, N. Harada, H. Nakamura, and Y. Habu, *Proc. 4th Process Tech. Conf.* (eds.), p.121, AIME, Chicago, USA (1984).
3. Y. Kato, K. Nakanishi, T. Nozaki, K. Suzuki, and T. Emi, *Tetsu-to-Hagane*, **68**, 1604 (1982).
4. N. Kikuchi, K. Yamaguchi, Y. Kishimoto, S. Takeuchi, and H. Mishikawa, *Tetsu-to-Hagane*, **88**, 450 (2002).
5. H. S. Sohn and K. H. Jung, *J. Kor. Inst. Met. & Mater.*, **47**, 107 (2009).
6. K. Sawamura, K. Mizoguchi, T. Hanada, and K. Makino, *Tetsu-to-Hagane*, **53**, 740 (1967).
7. H. S. Song, D. S. Kim, and C. H. Rhee, *85th Steelmaking Conf. Proc.*, p.301, ISS, Warrendale, PA, USA (2002).